

Rotational Relaxation of Hydrophobic Probes in Nonionic Reverse Micelles: Influence of Water Content on the Location and Mobility of the Probe Molecules

G. B. Dutt*

Radiation Chemistry & Chemical Dynamics Division, Bhabha Atomic Research Centre, Trombay, Mumbai 400 085, India

Received: September 8, 2003; In Final Form: November 6, 2003

Rotational relaxation studies of two structurally similar hydrophobic probes, 2,5-dimethyl-1,4-dioxo-3,6-diphenylpyrrolo[3,4-*c*]pyrrole (DMDPP) and 1,4-dioxo-3,6-diphenylpyrrolo[3,4-*c*]pyrrole (DPP), have been carried out in Triton X-100/cyclohexane (TX-100/cyclohexane) reverse micelles with increasing water content, $W = [\text{H}_2\text{O}]/[\text{TX-100}]$, in order to investigate the effect of added water on the location and mobility of the probe molecules. The anisotropy decays of both probes in the micelles have been adequately described by a sum of two exponentials with fast and slow reorientation times. The fast and slow components have been ascribed to the wobbling motion and the lateral diffusion of the probe in the micelle, respectively, and both of these motions are coupled to the rotation of the micelle as a whole. It has been observed that the average reorientation time $\langle\tau_r\rangle$ of DMDPP increases by a factor of 2 when W is increased from 0.0 to 4.2, and in case of DPP it is almost independent of W . These results have been rationalized on the basis of the differences in the chemical nature of the probe molecules, which enables them to interact with the micellar internal environment in a distinct manner.

1. Introduction

The dynamics of solute molecules confined in organized molecular assemblies has received considerable attention in recent times.^{1–3} These studies have enabled researchers to examine the nature of “biological water”, which exhibits different properties compared to bulk water. From several solvation dynamics studies in different kinds of organized media it has become evident that water molecules in the vicinity of supramolecular assemblies are immobilized because of their attachment to these assemblies via hydrogen bonds and hence display distinct characteristics compared to bulk water.³ While solvation dynamics studies in organized media essentially provide information regarding the dynamics of the medium around the solute molecule, rotational relaxation studies, on the other hand, probe the mobility of the solute molecule and hence furnish the details of the microenvironment surrounding it. To address this issue as to how the internal environment of an organized assembly influences the dynamics of a solute molecule solubilized in it, a number of rotational relaxation studies have been carried out in micelles^{4–11} and reverse micelles.^{12,13} In all of these studies probes were chosen in such a way that they are solubilized in the interfacial region of the micelles.

Although a number of solvation dynamics and quite a few rotational relaxation studies have been carried out in reverse micelles formed with ionic surfactants, only a handful of solvation dynamics studies in nonionic reverse micelles are available in the literature.^{14,15} Compared to reverse micelles formed with ionic surfactants where well-defined water droplets exist, the core of a nonionic reverse micelle does not contain water in the form of a pool; instead, it appears to be dispersed between the surfactant chains. Nonionic reverse micelles formed with the surfactant Triton X-100 (TX-100) in cyclohexane and in mixed solvents of benzene and *n*-hexane have been well characterized by Schelly and co-workers.^{16–21} According to their

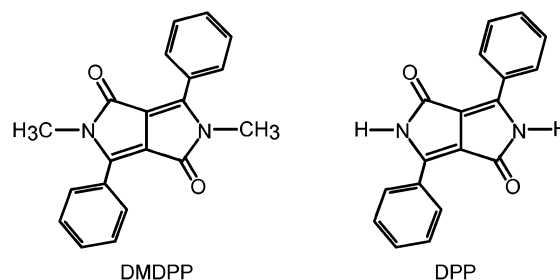


Figure 1. Molecular structures of the probes DMDPP and DPP.

findings, cyclohexane penetrates the polar interior of these aggregates, and upon the addition of water to the dry TX-100/cyclohexane reverse micelles, some of the cyclohexane molecules are displaced from the micellar core and water molecules hydrate the oxyethylene groups of the TX-100 surfactant chains. The number of water molecules that are bound to the oxyethylene chain was found to depend on the nature of the solvent used, and in case of cyclohexane, an average of 9.5 oxyethylene units of a TX-100 surfactant chain are hydrated by 5.5 water molecules.^{16,17} Even though the structure and micropolarity of the nonionic reverse micelles formed with TX-100 surfactant has been investigated thoroughly, very little information is available regarding the dynamical aspects of these micellar interiors apart from a few solvation dynamics studies reported in the literature.^{14,15} To the best of our knowledge, rotational relaxation studies, which are a convenient means of probing the microenvironment of these reverse micelles, are not available in the literature.

The present report deals with the rotational relaxation studies of two structurally similar hydrophobic probes, 2,5-dimethyl-1,4-dioxo-3,6-diphenylpyrrolo[3,4-*c*]pyrrole (DMDPP) and 1,4-dioxo-3,6-diphenylpyrrolo[3,4-*c*]pyrrole (DPP) (see Figure 1 for the molecular structures of the probes), solubilized in TX-100/cyclohexane reverse micelles as a function of the water content. The reasons for choosing the probes DMDPP and DPP are

* E-mail: gbdutt@apsara.barc.ernet.in.

manifold and are enumerated below. Both DMDPP and DPP are hydrophobic, and hence they will be solubilized only in the micellar phase. Despite having almost identical size and shape, DMDPP and DPP are chemically distinct. DPP, because of the presence of two secondary amino groups, forms different kinds of aggregates in the solid state through intermolecular hydrogen bonding²² and is soluble only in those solvents with which it can form hydrogen bonds at the two NH sites so that hydrogen bonding between the aggregates are broken. In view of its hydrogen-bonding nature, DPP is soluble only in the polar core of the TX-100/cyclohexane reverse micelles; DMDPP, on the other hand, is soluble in TX-100 as well as cyclohexane. Thus, the probes are expected to be solubilized in different regions of the micelle. A reasonably thorough understanding of the rotational dynamics of both of these probes in the condensed phase has been attained through numerous studies in homogeneous solvents^{23–30} as well as in nonionic micelles.^{7–9} Such an understanding will enable us to comprehend their dynamics in systems with an increasing degree of complexity like the one considered in the present study. Moreover, the fluorescence lifetimes of both the probes are relatively long, and hence anisotropy decays with long correlation times can be measured in a straightforward manner. We believe that all of these considerations make the probes DMDPP and DPP ideal choices for the present investigation. It will be interesting to find out how the location and the dynamics of the probes will be affected with an increase in the water content. The remainder of the paper is organized in the following manner. Section 2 describes the experimental methods used to measure the rotational diffusion of the probes in TX-100/cyclohexane reverse micelles. Results are presented in section 3 and are discussed in section 4. The conclusions of this work are summarized in the final section.

2. Experimental Section

The probes DMDPP and DPP are from Ciba Specialty Chemicals Inc., Switzerland. The surfactant TX-100 and spectroscopic grade cyclohexane are from BDH Chemicals Ltd., England and s. d. fine-chem Ltd., India, respectively. All the chemicals are of the highest available purity and were used as such. Deionized water from Millipore was used in the preparation of the micellar samples. Reverse micelles with different W values were prepared by weighing appropriate amounts of TX-100, cyclohexane, and water, and in all these samples the concentration of TX-100 was kept at 0.824 mol kg⁻¹. Care was taken to ensure that the concentrations of the probes were maintained in the range from 10⁻⁵ to 10⁻⁶ mol dm⁻³.

Steady-state anisotropies of the samples were measured using a Hitachi F-4010 spectrofluorometer, and the details have been described in our earlier publication.²³ The probes DMDPP and DPP were excited at 440 nm, and the emission was monitored in the range of 515–585 nm. Time-resolved fluorescence measurements were carried out using the time-correlated single-photon counting³¹ facility at the Tata Institute of Fundamental Research, Mumbai, India, and details of the system have been described elsewhere.²⁴ In brief, the frequency-doubled output of a picosecond Ti:sapphire laser (Tsunami, Spectra Physics) was used as the excitation source and the probes DMDPP and DPP were excited at 444 nm with a vertically polarized pulse. Fluorescence decays were collected at parallel ($I_{\parallel}(t)$), perpendicular ($I_{\perp}(t)$), and 54.7° ($I(t)$) orientations of the emission polarizer with respect to the polarization of the excitation radiation. The emission in all the three cases was monitored at 550 nm. For fluorescence lifetime measurements 10 000 peak counts were collected; in the case of anisotropy measurements

TABLE 1: Fluorescence Lifetimes and Anisotropy Decay Parameters of DMDPP in TX-100/Cyclohexane Reverse Micelles as a Function of the Water Content

W	τ_f /ns ^a	β	$\tau_{\text{slow}}/\text{ns}$	$\tau_{\text{fast}}/\text{ns}$	$\langle\tau_r\rangle/\text{ns}^b$	$\langle r \rangle/r_0^c$	$\langle r \rangle/r_0^d$
0.0	7.04	0.52 ± 0.02	1.4 ± 0.3	0.37 ± 0.06	0.9 ± 0.2	0.104	0.102
1.0	7.12	0.54 ± 0.02	1.7 ± 0.2	0.52 ± 0.07	1.2 ± 0.2	0.139	0.140
1.5	7.15	0.54 ± 0.01	1.9 ± 0.2	0.54 ± 0.03	1.3 ± 0.2	0.144	0.146
2.5	7.23	0.53 ± 0.03	2.2 ± 0.1	0.65 ± 0.09	1.5 ± 0.2	0.161	0.154
4.2	7.45	0.54 ± 0.04	2.4 ± 0.2	0.78 ± 0.08	1.7 ± 0.2	0.176	0.162

^a The maximum error in the fluorescence lifetimes is less than 2%.

^b Calculated using eq 2. ^c Calculated from the experimentally measured values of τ_f , τ_{slow} , τ_{fast} , and β using eq 3. ^d Obtained from the measured steady-state values of $\langle r \rangle$ and r_0 .

TABLE 2: Fluorescence Lifetimes and Anisotropy Decay Parameters of DPP in TX-100/Cyclohexane Reverse Micelles as a Function of the Water Content

W	τ_f /ns ^a	β	$\tau_{\text{slow}}/\text{ns}$	$\tau_{\text{fast}}/\text{ns}$	$\langle\tau_r\rangle/\text{ns}^b$	$\langle r \rangle/r_0^c$	$\langle r \rangle/r_0^d$
0.0	6.43	0.52 ± 0.02	5.1 ± 0.2	1.4 ± 0.2	3.3 ± 0.3	0.316	0.340
1.0	6.50	0.62 ± 0.02	5.4 ± 0.2	1.6 ± 0.3	4.0 ± 0.4	0.358	0.384
1.5	6.50	0.66 ± 0.01	5.7 ± 0.3	1.5 ± 0.1	4.3 ± 0.3	0.371	0.390
2.5	6.51	0.64 ± 0.03	5.8 ± 0.2	1.6 ± 0.2	4.3 ± 0.3	0.370	0.390
4.2	6.46	0.64 ± 0.02	5.4 ± 0.2	1.5 ± 0.2	4.0 ± 0.3	0.357	0.390

^a The maximum error in the fluorescence lifetimes is less than 2%.

^b Calculated using eq 2. ^c Calculated from the experimentally measured values of τ_f , τ_{slow} , τ_{fast} , and β using eq 3. ^d Obtained from the measured steady-state values of $\langle r \rangle$ and r_0 .

20 000 peak counts were collected for $I_{\parallel}(t)$ and $I_{\perp}(t)$ was corrected for the polarization bias or the G -factor of the spectrometer. The decays were collected in 512 channels with a time increment of 80 ps/channel. Each measurement was repeated at least 2 to 3 times, and the average values are reported. All measurements were performed at 298 K, and the sample temperature was maintained with the help of a temperature controller (Eurotherm).

The decays measured in this manner are convoluted with the instrument response function, which was measured by replacing the sample with a solution that scatters light. Lifetimes of the probes DMDPP and DPP in TX-100/cyclohexane reverse micelles were obtained from the fluorescence decays measured at magic angle polarization $I(t)$ and the instrument response function, by an iterative reconvolution method using the Marquardt algorithm as described by Bevington.³² Likewise, the anisotropy decay parameters were obtained by a simultaneous fit^{33,34} of the parallel $I_{\parallel}(t)$ and perpendicular $I_{\perp}(t)$ components. The criteria for a good fit were judged by statistical parameters such as a near unity value for the reduced χ^2 and a random distribution of the weighted residuals.

3. Results

3.A. Fluorescence Lifetimes. Fluorescence decays of DMDPP and DPP in TX-100/cyclohexane reverse micelles could be adequately described by single-exponential functions from $W = 0.0$ to 4.2. The lifetimes of DMDPP and DPP in TX-100/cyclohexane reverse micelles as a function of W are given in Tables 1 and 2, respectively. The lifetime τ_f of DMDPP increases from 7.04 to 7.45 ns with increasing water content. On the other hand, the lifetimes of DPP are around 6.50 ns and there is almost no variation of τ_f with W . DMDPP, unlike DPP, is also soluble in cyclohexane; hence, there exists a likely scenario that it may be solubilized in the cyclohexane surrounding the micelle as well as the micellar phase itself. To find out whether DMDPP is solubilized in cyclohexane or in the micellar phase, the lifetime of DMDPP was measured in cyclohexane

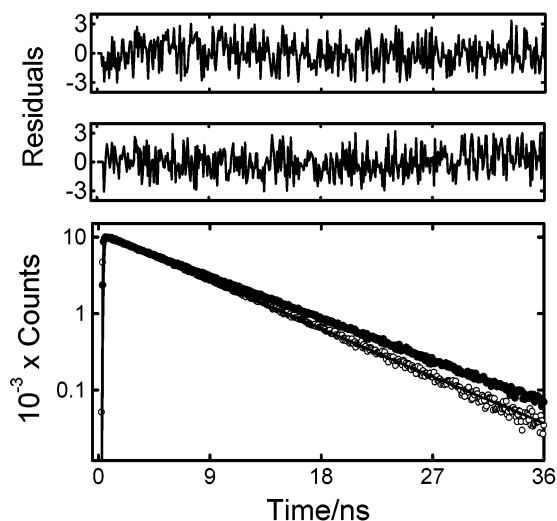


Figure 2. Fluorescence decays of DMDPP in cyclohexane (○) and in TX-100/cyclohexane reverse micelles (●). The solid lines were obtained by fitting the data to single-exponential functions; the lifetimes are 6.04 ns and 7.04 ns, respectively, in cyclohexane and in the reverse micelle. The lower and upper panels of the figure represent the residual distributions for cyclohexane and the reverse micelle, respectively. The instrument response function whose full-width at half-maximum is about 40 ps is not shown in the figure for the sake of clarity.

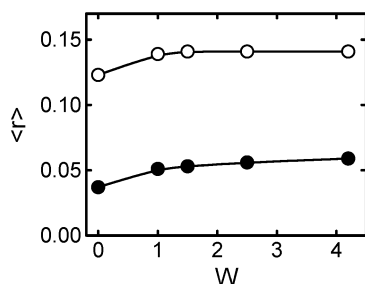


Figure 3. Plots of steady-state anisotropies of DMDPP (●) and DPP (○) in TX-100/cyclohexane reverse micelles at different values of W .

and was found to be 6.04 ns, which is shorter than the lifetimes reported in TX-100/cyclohexane reverse micelles, thus ruling out the possibility that DMDPP is solubilized in cyclohexane. Figure 2 shows the fluorescence decays of DMDPP in cyclohexane and in TX-100/cyclohexane reverse micelles at $W = 0.0$, and it is evident from the figure that there is a clear distinction between slopes of the two decays.

3.B. Steady-State Anisotropy. Figure 3 shows plots of steady-state anisotropy $\langle r \rangle$ versus W for both DMDPP and DPP in TX-100/cyclohexane reverse micelles. The value of $\langle r \rangle$ for DMDPP increases by 38% from $W = 0.0$ to 1.0; from $W = 1.0$ to 4.2 the increase is merely 16%. In the case of DPP, however, there is only a 15% increase in the value of $\langle r \rangle$ from $W = 0.0$ to 1.0, and it remains invariant with an increase in the value of W . These results may suggest that there is not much change in the internal environment of the TX-100/cyclohexane reverse micelles from $W = 1.0$ to 4.2. However, steady-state anisotropy is not a proper yardstick for arriving at such a conclusion as the value of $\langle r \rangle$ also depends on the fluorescence lifetimes of the probes. Analysis of the time-resolved anisotropy decays will give a better insight into the location and dynamics of the probe molecules.

3.C. Time-Resolved Anisotropy. Anisotropy decays of both DMDPP and DPP in TX-100/cyclohexane reverse micelles at all values of W could be adequately described by a sum of two exponentials whose functional form is given by the following

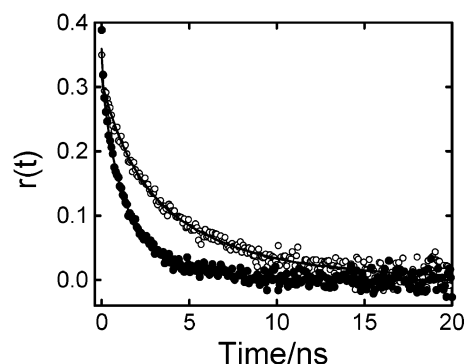


Figure 4. Anisotropy decays of DMDPP (●) and DPP (○) in TX-100/cyclohexane reverse micelles at $W = 4.2$. The smooth lines passing through them are the fitted ones. The average reorientation times, defined by eq 2, are 1.7 ns and 4.0 ns, respectively, for DMDPP and DPP.

equation.

$$r(t) = r_0 \left[\beta \exp\left(\frac{-t}{\tau_{\text{slow}}}\right) + (1 - \beta) \exp\left(\frac{-t}{\tau_{\text{fast}}}\right) \right] \quad (1)$$

Here, τ_{slow} and τ_{fast} are the two reorientation times associated with the slow and fast motions of the probe in the micelle, β is a pre-exponent which indicates the relative contributions of the slow and fast motions to the decay of the anisotropy, and r_0 is the limiting anisotropy. Typical anisotropy decays of DMDPP and DPP in TX-100/cyclohexane reverse micelles at $W = 4.2$ are shown in Figure 4. The anisotropy decay parameters of DMDPP and DPP in TX-100/cyclohexane reverse micelles as a function of W are given in Tables 1 and 2, respectively. The average reorientation times $\langle \tau_r \rangle$ that were calculated using the following equation are also given in the tables.

$$\langle \tau_r \rangle = \beta \tau_{\text{slow}} + (1 - \beta) \tau_{\text{fast}} \quad (2)$$

Inspection of the tables reveals that both τ_{slow} and τ_{fast} for DMDPP increase by a factor of 1.7 and 2.1, respectively, with an increase in the water content, whereas for DPP there is almost no change in either τ_{slow} or τ_{fast} values with W . The average reorientation times of DPP are significantly slower than those of DMDPP as a result of specific interactions between the two secondary amino groups of DPP and the poly(oxyethylene) chains of the TX-100 surfactant units. The ratio of the average reorientation time of DPP to DMDPP gradually decreases from 3.7 at $W = 0.0$ to 2.4 at $W = 4.2$. There are no changes in the β values for both probes with W , and the β values are around 0.5 and 0.6, respectively, for DMDPP and DPP.

To ensure that the anisotropy decay parameters recovered from the $I_{\parallel}(t)$ and $I_{\perp}(t)$ curves are accurate, they were compared with the steady-state anisotropies using the following relation.

$$\frac{\langle r \rangle}{r_0} = \left[\frac{\beta \tau_{\text{slow}}}{(\tau_f + \tau_{\text{slow}})} + \frac{(1 - \beta) \tau_{\text{fast}}}{(\tau_f + \tau_{\text{fast}})} \right] \quad (3)$$

Equation 3 is valid when the decay of the fluorescence is described by a single-exponential function and the anisotropy decay is described by a biexponential function as in the present case. It has been observed that the limiting anisotropy values obtained from the time-resolved experiments for both probes in TX-100/cyclohexane reverse micelles were found to be from 5% to 20% smaller than the true r_0 values obtained from the steady-state anisotropy measurements in glucose glass²³ as a result of some rapid depolarization of the fluorescence, which is beyond the time resolution of our single-photon counting

TABLE 3: Mean Hydrodynamic Radius r_h and τ_M Values of TX-100/Cyclohexane Reverse Micelles as a Function of the Water Content

W	r_h/nm^a	$\tau_M/\mu\text{s}^b$
0.0	10.7	1.1
1.0	30.5	26.0
1.5	29.5	23.5
2.5	25.6	15.4
4.2	22.3	10.1

^a r_h values were taken from ref 16. ^b τ_M values were calculated using eq 6.

setup. Only in the case of DPP in TX-100/cyclohexane at $W = 0.0$, an unusually low value of r_0 (0.20) has been obtained, which is probably due to some kind of fast segmental mobility of the TX-100 chains in the region where the probe DPP is intercalated. It is a well-known fact that added water molecules establish further bridges between the TX-100 chains inside the reverse micelle,¹⁶ which limit the segmental mobility, and hence higher values of r_0 were recovered upon the addition of water to the TX-100/cyclohexane reverse micelles. In view of these shortcomings, the quantity $\langle r \rangle/r_0$ instead of $\langle r \rangle$, obtained from the steady-state measurements, was compared with the one calculated using the parameters τ_f , τ_{slow} , τ_{fast} , and β recovered during the time-resolved analysis. The $\langle r \rangle/r_0$ values obtained using these two approaches are also given in Tables 1 and 2, respectively, for DMDPP and DPP. The agreement between the two sets of $\langle r \rangle/r_0$ values is within 10%, indicating that the parameters recovered from the time-resolved anisotropy decay curves are indeed accurate.

4. Discussion

To comprehend these intriguing results, a thorough understanding of the micellar structure and the location of the probe within the micelle are mandatory. As mentioned briefly in the Introduction, Schelly and co-workers^{16,17} have characterized TX-100/cyclohexane reverse micelles at different values of W . Their findings indicate that these micelles are not spherical, and the mean hydrodynamic radius r_h of dry TX-100/cyclohexane reverse micelles is 10.7 nm at 298 K. The r_h increases upon the addition of water until $W = 1.0$ and then decreases with further increase in W . Table 3 gives the changes in r_h values as a function of W for TX-100/cyclohexane reverse micelles, which were taken from ref 16. The complex pattern observed in the r_h values is due to a combination of the delicate balance between the multitude of molecular interactions and the geometrical constraints.¹⁶ The microenvironments of TX-100/cyclohexane reverse micelles have been investigated using methyl orange as a probe, and it was found that in dry TX-100 reverse micelle, cyclohexane penetrates the polar interior of the aggregates in such a way that the molar ratio of cyclohexane/TX-100 is about 4.5. This ratio decreases to about 3.0 at $W = 2.5$ as the added water displaces some of the cyclohexane molecules from the core; it was also found that these water molecules do not form a pool, but instead they are dispersed between the poly-(oxyethylene) chains.¹⁷

From the results presented in the previous section it can be postulated that both probes are solubilized in the polar interior of the TX-100/cyclohexane reverse micelles. Because the average length of the hydrophilic part of the TX-100 surfactant chain is about 17 Å³⁵ and also the fact that the probes are chemically distinct, there exists a possibility that the probes DMDPP and DPP may be solubilized in different regions of the polar interior. A detailed analysis of the anisotropy data will provide conclusive evidence for such a hypothesis. The

TABLE 4: Order Parameters, Cone Angles, and Wobbling Diffusion Coefficients for DMDPP and DPP in TX-100/Cyclohexane Reverse Micelles Obtained from the Analysis of the Anisotropy Decays

W	DMDPP			DPP		
	S	θ^0	$D_W \times 10^{-8}/\text{s}^{-1}$	S	θ^0	$D_W \times 10^{-8}/\text{s}^{-1}$
0.0	0.72	36.9	2.1	0.72	36.8	0.55
1.0	0.73	36.1	1.4	0.79	31.5	0.35
1.5	0.73	36.1	1.4	0.81	29.8	0.36
2.5	0.73	36.1	1.1	0.80	30.7	0.35
4.2	0.73	36.1	0.9	0.80	30.7	0.36

observed biexponential anisotropy decays of the probes in micelles are usually explained^{4–10} using a two step model^{36–39} consisting of slow lateral diffusion of the probe on the surface of the micelle and fast wobbling motion of the probe in the micelle that are coupled to the overall rotation of the micelle. Assuming that the slow and fast motions are separable, the following expressions can be used to relate experimentally measured quantities and model parameters.

$$\frac{1}{\tau_{\text{slow}}} = \frac{1}{\tau_L} + \frac{1}{\tau_M} \quad (4)$$

$$\frac{1}{\tau_{\text{fast}}} = \frac{1}{\tau_W} + \frac{1}{\tau_{\text{slow}}} \quad (5)$$

Here, τ_L and τ_W are the time constants for the lateral diffusion and the wobbling motion of the probe, respectively. τ_M is the time constant for the overall rotation of the micelle and can be estimated using the Stokes–Einstein–Debye relation⁴⁰ with the stick boundary condition.

$$\tau_M = \frac{4\pi r_h^3 \eta}{3kT} \quad (6)$$

In the above expression, η is the viscosity of cyclohexane and k and T are the Boltzmann constant and absolute temperature, respectively. However, it must be noted that because the TX-100/cyclohexane reverse micelles are nonspherical, the τ_M value obtained using eq 6 is only a rough estimate of the time constant for the rotation of the micelle but not its exact value. The calculated τ_M values are given in Table 3, and it can be inferred from the table that the reorientation times of the TX-100/cyclohexane reverse micelles are in the range of a few microseconds; hence, the overall rotation of the micelle does not contribute to the decay of the anisotropy. In view of this, τ_{slow} and τ_{fast} essentially represent the time constants for lateral diffusion and wobbling motion, respectively.

The generalized order parameter S , whose magnitude is considered a measure of the spatial restriction of the probe and which can have values from zero for unrestricted rotation of the probe to one for completely restricted motion, is obtained from β using the relation³⁶

$$\beta = S^2 \quad (7)$$

The values of the order parameters for the probes DMDPP and DPP in TX-100/cyclohexane reverse micelles are around 0.7 and 0.8 (see Table 4), respectively, and are almost independent of W . These kinds of high values for the order parameters indicate that the probes are experiencing restricted rotation in the micelles. Now the question that can be asked is where exactly are the probes located in the micelles so as to experience restricted rotation. To experience restricted rotation, both probes need to be solubilized in the core of the TX-100/cyclohexane

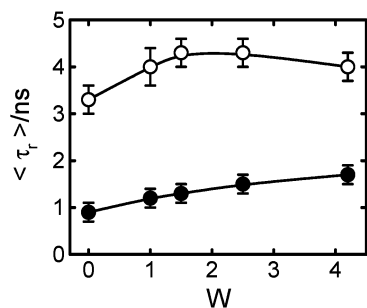


Figure 5. Plot of $\langle \tau_r \rangle$ vs W for DMDPP (●) and DPP (○) in TX-100/cyclohexane reverse micelles. The lines through the experimental points are drawn as a visual aid.

reverse micelles where the poly(oxyethylene) chains of the TX-100 that exist in the form of a random coil or in meander conformation³⁵ do not allow isotropic rotational diffusion of the probes. However, it is not feasible to pinpoint the exact location of the probes within the core of the TX-100/cyclohexane reverse micelles from the values of the order parameters.

In dry TX-100/cyclohexane reverse micelles DMDPP is solubilized in the core together with the cyclohexane molecules because cyclohexane penetrates the polar core.¹⁷ As water is added to the reverse micelles, some of the cyclohexane molecules are pushed away from the core, which increases the microviscosity of the region where DMDPP is located, and hence the mobility of the probe molecule decreases. This is consistent with the experimentally observed trend in the average reorientation times of DMDPP, which increase by almost a factor of 2 from $W = 0.0$ to $W = 4.2$. In contrast, DPP, which is not soluble in cyclohexane, is located in the interior of the core where cyclohexane molecules are absent. Hence, addition of water and depletion of some of the cyclohexane molecules from the core of the reverse micelles does not have any effect on the dynamics of DPP. This has been reflected in the average reorientation times, which are, with the exception of $\langle \tau_r \rangle$ at $W = 0.0$, independent of the water content. Figure 5 gives plots of average reorientation times of DMDPP and DPP at different values of W . Further justification for these arguments comes from the average reorientation times of DMDPP and DPP obtained in TX-100 micelles in water.⁷ The $\langle \tau_r \rangle$ value of DMDPP in TX-100 micelles at 298 K, where the probe is solubilized in the interfacial region of the micelle, is 2.56 ns, which is very different from the values obtained in TX-100/cyclohexane reverse micelles. In the case of DPP, however, $\langle \tau_r \rangle$ is 4.35 ns and is almost identical to the values obtained in the TX-100/cyclohexane reverse micelles indicating that the probe DPP experiences the same microenvironment in the TX-100 micelles as in the reverse micelles.

Having established the location of the probes in these micelles, we now discuss the slow and fast time constants obtained from the time-resolved anisotropy decays in detail. As mentioned earlier, τ_{slow} represents the time constant for lateral diffusion and is related to the lateral diffusion coefficient by the relation⁵

$$D_L = \frac{r^2}{6\tau_L} \quad (8)$$

In the above expression, r represents the radius of the curved micellar surface on which the probe diffuses or translates. In the present scenario, because lateral diffusion of the probe is taking place in the core of the micelles, the mean hydrodynamic radius r_h of the TX-100/cyclohexane reverse micelle cannot be

employed to obtain the lateral diffusion coefficient. The fact that the radius of the curved surface on which lateral diffusion of the probes occurs is not obtainable precludes the estimation of the lateral diffusion coefficients.

The information pertinent to wobbling motion is contained in τ_{fast} . According to the wobbling-in-cone model, the probe molecules wobble freely inside a cone of semiangle θ , which can be obtained from the order parameter using the following equation.³⁶

$$S = 0.5 \cos \theta (1 + \cos \theta) \quad (9)$$

The diffusion coefficients for wobbling motion D_W were calculated from τ_W , S , and θ using the relation³⁸

$$D_W = \frac{1}{[(1 - S^2)\tau_W]} \left[\frac{\cos^2 \theta (1 + \cos \theta)^2}{2(\cos \theta - 1)} \left\{ \ln \left(\frac{1 + \cos \theta}{2} \right) + \frac{(1 - \cos \theta)}{2} \right\} + \frac{(1 - \cos \theta)}{24} (6 + 8 \cos \theta - \cos^2 \theta - 12 \cos^3 \theta - 7 \cos^4 \theta) \right] \quad (10)$$

The cone angles and the D_W values obtained from eqs 9 and 10 for both probes are also given in Table 4. It can be observed from the table that the diffusion coefficients for wobbling motion are significantly higher for DMDPP compared to DPP. This is due to the specific interactions between the probe DPP and poly(oxyethylene) chains of the surfactant TX-100, which slow the wobbling motion of the probe, and is consistent with our earlier results in TX-100 and Brij-35 micelles.⁷⁻⁹ The D_W value of DMDPP decreases with increasing water content indicating that the microviscosity experienced by the probe increases because of the decrease in the number of cyclohexane molecules in the core. On the other hand, the D_W values of DPP, except for the one at $D_W = 0.0$, remain the same, as the probe is located in an environment that is free from cyclohexane, and hence do not vary with increasing water content.

5. Conclusions

Nonionic surfactants, unlike their ionic counterparts, have long hydrophilic segments, and it has been well established that the cores of the reverse micelles formed with these surfactants have a propensity to accommodate both water as well as the nonpolar solvent. Reverse micelles of TX-100 in cyclohexane with different amounts of water belong to such category, and their structure has been investigated thoroughly. However, not much is known about the internal environment that influences the dynamics of probe molecules solubilized in the cores of these reverse micelles. The task of exploring the micellar internal environment can be accomplished by judiciously choosing the probes and studying their rotational relaxation. The present study is one such attempt in that direction, and to this effect the rotational relaxation of two structurally similar solutes, DMDPP and DPP, has been investigated in TX-100/cyclohexane reverse micelles with increasing water content. The important conclusions from this study are as follows. It has been established from their chemical properties and fluorescence lifetime data that DMDPP and DPP are located in the core of the reverse micelles. Analysis of the time-resolved anisotropy data reveals that the probe DMDPP is solubilized in a region where both cyclohexane and poly(oxyethylene) units are present. As water is added to the system, the average reorientation time, which is an indicator of its mobility, increases due to the removal of some of the cyclohexane molecules from the core. In other

words, the microviscosity around DMDPP increases. In contrast to DMDPP, DPP is solubilized in a location of the core that is devoid of both cyclohexane and water. This has been substantiated by the fact that DPP is experiencing the same microenvironment in TX-100/cyclohexane reverse micelles as in aqueous TX-100 micelles, which is evident from its average reorientation times that are identical in both the cases. In the case of aqueous TX-100 micelles, it has been established from the correlation of the lateral diffusion coefficients of the probes with the "dry" micelle radii⁸ that the site of solubilization of the probes is not surrounded by water. Such an outcome enables us to conclude that DPP is located in the "dry" area even in the case of TX-100/cyclohexane reverse micelles. Hence, addition of water and removal of some of the cyclohexane molecules from the core does not have any effect on its dynamics. In essence, the microenvironment surrounding DPP, unlike that of DMDPP, essentially remains the same with increasing water content. The findings of this work illustrate that there are several different interior areas, as opposed to a featureless interior in these nonionic reverse micelles.

Acknowledgment. I am grateful to Ms. M. H. Kombrabail of the Tata Institute of Fundamental Research for her help with the time-resolved fluorescence experiments. I thank Dr. P. N. Bajaj, Dr. T. Mukherjee, and Dr. J. P. Mittal for their encouragement throughout the course of this work.

References and Notes

- (1) Bhattacharyya, K.; Bagchi, B. *J. Phys. Chem. A* **2000**, *104*, 10603.
- (2) Pal, S. K.; Peon, J.; Bagchi, B.; Zewail, A. H. *J. Phys. Chem. B* **2002**, *106*, 12376.
- (3) Bhattacharyya, K. *Acc. Chem. Res.* **2003**, *36*, 95.
- (4) Quitevis, E. L.; Marcus, A. H.; Fayer, M. D. *J. Phys. Chem.* **1993**, *97*, 5762.
- (5) Maiti, N. C.; Krishna, M. M. G.; Britto, P. J.; Periasamy, N. *J. Phys. Chem. B* **1997**, *101*, 11051.
- (6) Krishna, M. M. G.; Das, R.; Periasamy, N.; Nityananda, R. *J. Chem. Phys.* **2000**, *112*, 8502.
- (7) Dutt, G. B. *J. Phys. Chem. B* **2002**, *106*, 7398.
- (8) Dutt, G. B. *J. Phys. Chem. B* **2003**, *107*, 3131.
- (9) Dutt, G. B. *J. Phys. Chem. B* **2003**, *107*, 10546.
- (10) Kelepouris, L.; Blanchard, G. J. *J. Phys. Chem. B* **2003**, *107*, 1079.
- (11) Delacruz, J. L.; Blanchard, G. J. *J. Phys. Chem. B* **2003**, *107*, 7102.
- (12) Visser, A. J. W. G.; Vos, K.; Hoek, A. V.; Santems, J. S. *J. Phys. Chem.* **1988**, *92*, 759.
- (13) Wittouck, N.; Negri, R. M.; Ameloot, M.; De Schryver, F. C. *J. Am. Chem. Soc.* **1994**, *116*, 10601.
- (14) Mandal, D.; Datta, A.; Pal, S. K.; Bhattacharyya, K. *J. Phys. Chem. B* **1998**, *102*, 9070.
- (15) Pant, D.; Levinger, N. E. *Langmuir* **2000**, *16*, 10123.
- (16) Zhu, D.-M.; Feng, K.-I.; Schelly, Z. A. *J. Phys. Chem.* **1992**, *96*, 2382.
- (17) Zhu, D.-M.; Schelly, Z. A. *Langmuir* **1992**, *8*, 48.
- (18) Zhu, D.-M.; Wu, X.; Schelly, Z. A. *Langmuir* **1992**, *8*, 1538.
- (19) Zhu, D.-M.; Wu, X.; Schelly, Z. A. *J. Phys. Chem.* **1992**, *96*, 7121.
- (20) Gu, J.; Schelly, Z. A. *Langmuir* **1997**, *13*, 4251.
- (21) Gu, J.; Schelly, Z. A. *Langmuir* **1997**, *13*, 4256.
- (22) Adachi, M.; Nakamura, S. *J. Phys. Chem.* **1994**, *98*, 1796.
- (23) Dutt, G. B.; Srivatsavoy, V. J. P.; Sapre, A. V. *J. Chem. Phys.* **1999**, *111*, 9705.
- (24) Dutt, G. B.; Srivatsavoy, V. J. P.; Sapre, A. V. *J. Chem. Phys.* **1999**, *110*, 9623.
- (25) Dutt, G. B.; Krishna, G. R. *J. Chem. Phys.* **2000**, *112*, 4676.
- (26) Dutt, G. B. *J. Chem. Phys.* **2000**, *113*, 11154.
- (27) Dutt, G. B.; Ghanty, T. K. *J. Chem. Phys.* **2002**, *116*, 6687.
- (28) Dutt, G. B.; Ghanty, T. K. *J. Chem. Phys.* **2003**, *118*, 4127.
- (29) Dutt, G. B.; Sachdeva, A. *J. Chem. Phys.* **2003**, *118*, 8307.
- (30) Dutt, G. B.; Ghanty, T. K. *J. Chem. Phys.* **2003**, *119*, 4768.
- (31) O'Connor, D. V.; Phillips, D. *Time-Correlated Single Photon Counting*; Academic Press: London, 1984.
- (32) Bevington, P. R. *Data Reduction and Error Analysis for the Physical Sciences*; McGraw-Hill: New York, 1969.
- (33) Cross, A. J.; Fleming, G. R. *Biophys. J.* **1984**, *46*, 45.
- (34) Knutson, J. R.; Beechem, J. M.; Brand, L. *Chem. Phys. Lett.* **1983**, *102*, 501.
- (35) Robson, R. J.; Dennis, E. A. *J. Phys. Chem.* **1977**, *81*, 1075.
- (36) Lipari, G.; Szabo, A. *Biophys. J.* **1980**, *30*, 489.
- (37) Lipari, G.; Szabo, A. *J. Chem. Phys.* **1981**, *75*, 2971.
- (38) Lipari, G.; Szabo, A. *J. Am. Chem. Soc.* **1982**, *104*, 4546.
- (39) Szabo, A. *J. Chem. Phys.* **1984**, *81*, 1984.
- (40) Debye, P. *Polar Molecules*; Dover: New York, 1929.